Observations of Sidewall Domain Structures in Magnetic Grating

JinBae Kim[1,2], Jae-Hwang Lee[3], and Jongryoul Kim[1]

[1]Department of Metallurgy and Materials Engineering, Hanyang University, Ansan 426-791, Korea
[2]Research Institute of Engineering and Technology, Hanyang University, Ansan 426-791, Korea
[3]Department of Materials Science and Engineering, Massachusetts Institute of Technology, Cambridge, MA 02139 USA

In this paper, we demonstrate the direct observation of closure-type domain structures in Ni magnetic grating by employing conventional magnetic force microscopy (MFM) and tilt-scanning (TS) MFM. Through sidewall scanning, the TS-MFM operation enabled the detailed analysis of the spin configurations of head-to-head and tail-to-tail domains. As a result, the domains had the surface domain configurations of the closure-type structures, which was in accord with micromagnetic simulated results.

***Index Terms*—Magnetic domains, magnetic force microscopy (MFM), magnetic grating.**

I. Introduction

INTEGRATION of patterned magnetic media has become one of key issues in recent years because of their potential application to information technology, which utilizes optical and magnetic storage devices [1]–[4]. Recent results demonstrated the enhancement of the magnetic-optical effect in the patterned media [5]–[7]. Consequently, an interest in the micromagnetic structures and the evolution of magnetic domains has been sharply increased. In particular, the domain structures at remanent states after various magnetic histories are also crucial for the integration limits of magnetic memories and patterned recording media [3], [4].

In the past several decades, there have been a number of investigations utilizing various imaging techniques to elucidate the magnetic domain structures. Conventional magnetic force microscopy (MFM) is an imaging technique based on atomic force microscopy (AFM), in which magnetic forces (or force gradients) are measured to obtain the domain pattern images of ferromagnetic samples with high spatial resolution down to about 10 nm [8], [9]. In addition, MFM can be easily operated under various environmental conditions, requires little sample preparation, and is a nondestructive technique. Thus, MFM has received remarkable attention for the magnetic storage application in magnetic films. However, most of the previous studies on the magnetic domain structures in periodic structures based on patterned magnetic media have not included any experimental observations of sidewall domain structures. A full understanding of magnetic domains arrangement is necessary for future applications. Recently, we observed the spin configurations of vertical Bloch line structures in a ferromagnetic MnAs film on GaAs(001) by tilt-scanning (TS) MFM [10]. This attribute of TS-MFM can enable the magnetization mapping of sidewall magnetic domain structures in magnetic grating. In this study, we present the direct observation of spin configurations in Ni magnetic grating, investigated by conventional MFM and TS-MFM.

Manuscript received February 21, 2011; accepted April 17, 2011. Date of current version September 23, 2011. Corresponding author: J. Kim (e-mail: jina@hanyang.ac.kr).

Color versions of one or more of the figures in this paper are available online at http://ieeexplore.ieee.org.

Digital Object Identifier 10.1109/TMAG.2011.2147292

II. Experimental Work

In order to fabricate magnetic Ni grating structures on glass substrates, we employed a soft-lithography technique, the so-called two-polymer-microtransfer molding [11]. This technique was proven to have a number of advantages, including low cost, capability for nonperiodic 3-D structures, a wide range of material compatibility, and flexibility in design.

The magnetic domain structures were observed using conventional MFM and TS-MFM systems (Park systems) with magnetic tips (nanosensors). The longitudinal Kerr rotation was measured at 45° incidence by using a photoelastic modulator method. In order to conceptualize sidewall magnetic domain imaging, a z-scanner was tilted at 55° from the vertical axis of the conventional MFM. The magnetic tip scanned the sample in the noncontact mode to obtain the surface morphology and then a second scan was carried out at a constant height above the surface for the separation of the magnetic and the topographic signals. All MFM images were obtained in the interleave mode at a lift scan height of 50 nm.

III. Results and Discussion

The magnetization reversal of Ni magnetic grating was investigated by magneto-optical Kerr effect measurements. The inset image in Fig. 1 shows the AFM image of the Ni magnetic grating in which the observation area was $10 \times 10\ \mu m^2$. Fig. 1 shows normalized Kerr rotation hysteresis loops for two different field directions measured at room temperature. The external magnetic field (H) was applied both parallel $[H$ (i)] and perpendicular $[H$ (ii)] to the groove direction, which are indicated by the white arrows in Fig. 1. A magnetic easy-axis-like hysteresis loop was obtained when the orientation of H was parallel to the long side of rectangles [12]. This result can be explained by an enhanced surface effect with shape anisotropy.

Fig. 2(a) shows the conventional MFM phase overlaid on AFM height image of a Ni magnetic grating, where the observed area was $10 \times 10\ \mu m^2$. The width and depth of the groove were set to be 1.2 μm, and 0.6 μm, respectively. The overlaid image in Fig. 2(a) clearly shows a stripe pattern which corresponds to alternating magnetic and nonmagnetic regions in the sample with the same periodicity of about 2.6 μm, confirmed by the line profile of an AFM signal across the stripe [Fig. 2(b)]. The correlation between the spin directions in the domains of the neighborhood ferromagnetic stripes seems to be no correlation. This

0018-9464/$26.00 © 2011 IEEE

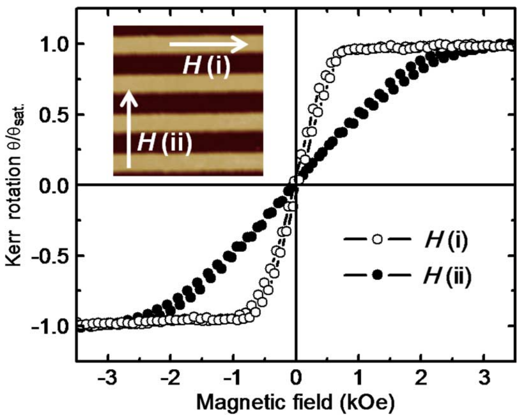

Fig. 1. Measured hysteresis loops, in which an external field is applied along the H (i) and along the H (ii) direction.

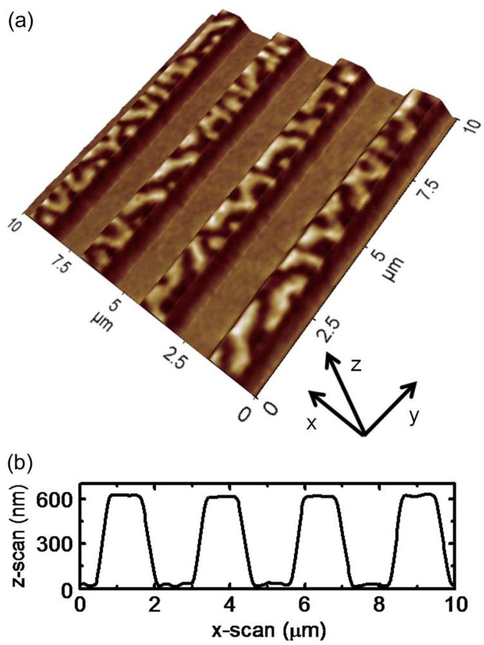

Fig. 2. (a) Conventional MFM phase overlaid on AFM height image of a Ni magnetic grating. (b) Line profile of conventional AFM signal across the stripe.

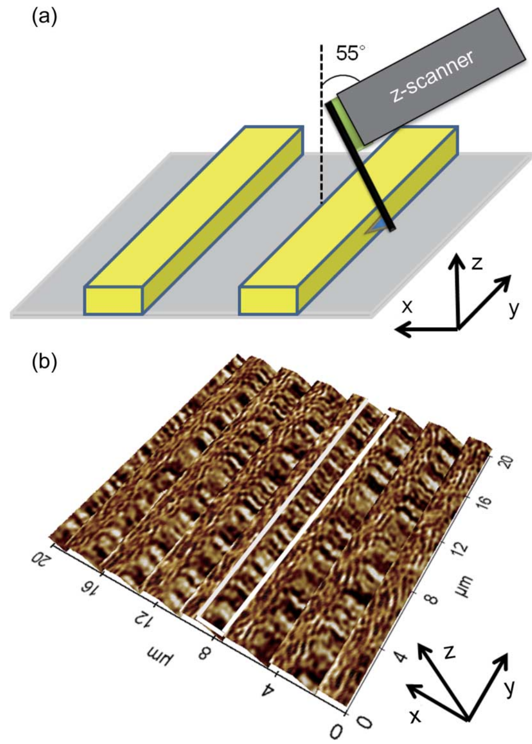

Fig. 3. (a) Schematic diagram of a Ni magnetic grating by TS-MFM. (b) TS-MFM phase overlaid on AFM height image of a Ni magnetic grating. The observed vertical domain structures in the white rectangular area defined in (b).

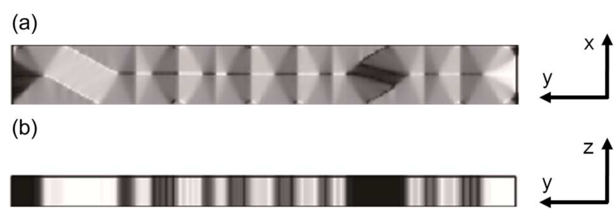

Fig. 4. Snapshots of the micromagnetic simulation of static magnetization configurations on a Ni bar at different geometry: (a) xy-plane and (b) yz-plane.

is due to the large gap that reduces the dipolar interaction. In the remanent state, the Ni magnetic grating exhibits rather complex magnetic domain patterns consisting of sawtooth shaped and elongated domains. It should be noted that the MFM contrast within a ferromagnetic Ni stripe is due to the stray field from the end parts of the in-plane magnet. As seen in Fig. 2(a), the domain structure can be described as a mixture of closure-type domain structures [13]. This indicates that the in-plane magnetization directions of the stripe domains are parallel or antiparallel to the easy magnetic axis. In systems with a negligible magneto-crystalline anisotropy, the balance of demagnetization and exchange energies results in closure structures. However, conventional MFM is known to have a lateral scan result as it has not directly analyzed vertical plane magnetic domain structures, as seen in Fig. 2(a).

In order to perform a sidewall stray magnetic field imaging, the z-scanner is tilted at 55° from the vertical axis of conventional MFM. The measurement system is shown schematically in Fig. 3(a). TS-MFM shows the sidewall magnetic domain structures of Ni magnetic grating [see Fig. 3(b)]. The TS-MFM image shows a stripe-like pattern that corresponds to the alternating dark- and bright-band regions. It should be also stressed that the magnetization directions are parallel to the stripe direction of two nearest-neighbor domains in the sidewall domain configuration, as presented in the white box of Fig. 3(b). The domain structure within the sidewall ferromagnetic stripes contains a mixture of head-to-head and tail-to-tail domains. This structure generates the magnetic charge density along the stripe direction. Thus, it is concluded that the head-on domain structures observed at sidewall domain represent the surface domain configurations of the closure-type structures.

An image in Fig. 4 demonstrates simulated domain patterns. The micromagnetic simulation was carried out using the object oriented micromagnetic framework (OOMMF) software for a 0.6-μm thickness, 10-μm length, and 1.2-μm width, with an in-plane uniaxial anisotropy [14]. The input material parameters of Ni were chosen: magnetization at saturation $M_s = 490 \times 10^3$ A/m, exchange constant $A = 9 \times 10^{-11}$ J/m, and magneto-crystalline anisotropy constant $K_1 = 3.5 \times 10^3$ J/m^3. Fig. 4(a) shows the closure-domain structures of a Ni bar. According to our simulations, as shown in Fig. 4(b), the domain structural characteristics could not be detected using conventional MFM, although the TS-MFM image in Fig. 3(b) evidently suggests the magnetization direction parallel to the stripe direction of two nearest-neighbor domains. As shown in Fig. 4, the overall agreement between the experiment and the micromagnetic simulation is indeed remarkable. It is clearly suggested that the Ni grating has the closure-type domain structures. The state at $H = 0$ is a typical feature of the closure domain structure, which is caused by its magnetostatic energy minimization process [15]–[17].

IV. Conclusion

We present the direct observation of the spin configurations in Ni magnetic grating, investigated by conventional MFM and TS-MFM. The TS-MFM image showed that the type of domain structure was a stripe-like pattern which corresponded to the alternating dark- and bright-band regions. Using TS-MFM, this domain structures was proven to represent the surface domain configurations of the closure-type structures, which was also confirmed by OOMMF simulation.

Acknowledgment

This work was supported by the research fund of Hanyang University, Korea, under Grant HY-2009-N.

References

[1] C. A. Ross, “Patterned magnetic recording media,” *Annu. Rev. Mater. Res.*, vol. 31, pp. 203–235, 2001.

[2] I. L. Lyubchanskii, N. N. Dadoenkova, M. I. Lyubchanskii, E. A. Shapovalov, and T. Rasing, “Magnetic photonic crystals,” *J. Phys. D, Appl. Phys.*, vol. 36, pp. R277–R287, 2003.

[3] A. Moser, K. Takano, D. T. Margulies, M. Albrecht, Y. Sonobe, Y. Ikeda, S. Sun, and E. E. Fullerton, “Magnetic recording: Advancing into the future,” *J. Phys. D, Appl. Phys.*, vol. 35, pp. R157–R167, 2002.

[4] B. D. Terris and T. Thomson, “Nanofabricated and self-assembled magnetic structures as data storage media,” *J. Phys. D, Appl. Phys.*, vol. 38, pp. R199–R222, 2005.

[5] R. Antos, J. Mistik, T. Yamaguchi, S. Visnovsky, S. O. Demokritov, and B. Hillebrands, “Evidence of native oxides on the capping and substrate of permalloy gratings by magneto-optical spectroscopy in the zeroth and first-diffraction orders,” *Appl. Phys. Lett.*, vol. 86, p. 231101, 2005.

[6] J. B. Kim, G. J. Lee, Y. P. Lee, J. Y. Rhee, K. W. Kim, and C. S. Yoon, “One-dimensional magnetic grating structure made easy,” *Appl. Phys. Lett.*, vol. 89, p. 151111, 2006.

[7] J. B. Kim, Y. H. Lu, M. H. Cho, G. J. Lee, Y. P. Lee, J. Y. Rhee, and C. S. Yoon, “Diffracted magneto-optical Kerr effect in one-dimensional magnetic gratings,” *Appl. Phys. Lett.*, vol. 94, p. 151110, 2009.

[8] J. J. Sáenz, N. García, P. Grütter, E. Meyer, H. Heinzelmann, R. Wiesendanger, L. Rosenthaler, H. R. Hidber, and H.-J. Güntherodt, “Observation of magnetic forces by the atomic force microscope,” *J. Appl. Phys.*, vol. 62, pp. 4293–4295, 1987.

[9] M. R. Freeman and B. C. Choi, “Advances in magnetic microscopy,” *Science*, vol. 294, pp. 1484–1488, 2001.

[10] J. B. Kim, H. Akinaga, and J. Kim, “Direct observation of the spin configurations of vertical Bloch line,” *Appl. Phys. Lett.*, vol. 98, p. 052510, 2011.

[11] J.-H. Lee, C.-H. Kim, K. Constant, and K.-M. Ho, “Two-polymer microtransfer molding for highly layered microstructures,” *Adv. Mater.*, vol. 17, pp. 2481–2485, 2005.

[12] K. Temst, E. Popova, M. J. Van Bael, H. Loosvelt, J. Swerts, D. Buntinx, Y. Bruynseraede, C. Van Haesendonck, H. Fritzsche, M. Gierlings, L. H. A. Leunissen, and R. Jonckheere, “Magnetization reversal in patterned ferromagnetic and exchange-biased nanostructures studied by neutron reflectivity,” *J. Appl. Phys.*, vol. 97, p. 10K117, 2005.

[13] A. Hubert and R. Schäfer, *Magnetic Domains*. Berlin, Germany: Springer-Verlag, 1998.

[14] “A 2D code to calculate the magnetization configuration and its field evolution,” [Online]. Available: http:/math.nist.gov/oommf

[15] H. Shima, K. Y. Guslienko, V. Novosad, Y. Otani, K. Fukamichi, N. Kikuchi, O. Kitakami, and Y. Shimada, “Magnetization reversal in magnetostatically coupled dot arrays,” *J. Appl. Phys.*, vol. 91, pp. 6952–6954, 2002.

[16] V. Novosad, M. Grimsditch, K. Y. Guslienko, P. Vavassori, Y. Otani, and S. D. Bader, “Spin excitations of magnetic vortices in ferromagnetic nanodots,” *Phys. Rev. B*, vol. 66, 2002, 052407.

[17] A. Kobs, H. Spahr, D. Stickler, S. Hankemeier, R. Frömter, and H. P. Oepen, “Magnetic energies of single submicron permalloy rectangles determined via magnetotransport,” *Phys. Rev. B*, vol. 80, p. 134415, 2009.